There is excellent agreement between calculated and experimental H^E at 298.15 K. The $\sigma(H^E)$ values at 313.15 K are larger but still quite satisfactory (Figure 2).

Preliminary measurements and calculations for dichloromethane (CH_2Cl_2) + 1-chloroalkane mixtures show that the dispersive coefficients $C^{dis}_{d'd'',1}$ are more negative than for 1,2-dichloroethane + 1-chlorobutane. The parameters of the whole series of α,ω-dichloroalkane + 1-chloroalkane mixtures will be published in the near future.

Glossary

A_j	parameters in eqs 1 or 3
B_{ij}	molar second virial coefficients, $cm^3\ mol^{-1}$
C	interchange coefficient
G	molar Gibbs energy, $J\ mol^{-1}$
H	molar enthalpy, $J\ mol^{-1}$
m	number of parameters A_j, eqs 1 or 3
N	total number of measurements
n	number of C atoms in chloroalkane
P	total vapor pressure, Pa
Q	any property
R	molar gas constant (8.314 51 $J\ K^{-1}\ mol^{-1}$)
S	objective function, ref 12
T	temperature, K
V	liquid molar volume, $cm^3\ mol^{-1}$
WRMSD	weighted root mean square deviation, eq 4
x	liquid mole fraction
y	vapor mole fraction

Greek Letters

ρ	liquid density, $g\ cm^{-3}$
$\sigma(Q)$	standard deviation of property Q, eq 5
$\sigma_m(Q)$	standard deviation of property Q, eq 2
σ_e	experimental uncertainty

Superscripts

dis	dispersive term
E	excess property
quac	quasi-chemical term
°	pure component

Subscripts

Az	azeotropic property
calc	calculated property
i	type of molecule (component)
a, d, d', d''	type of contact surface: a, aliphatic; d, Cl in CCl_4; d', Cl in 1-chloroalkane; d'', Cl in 1,2-dichloroethane
l	order of interchange coefficient; $l = 1$, Gibbs energy; $l = 2$, enthalpy
s, t	any contact surface

Registry No. $CH_3(CH_2)_2CH_2Cl$, 109-69-3; CCl_4, 56-23-5; $ClCH_2CH_2Cl$, 107-06-2.

Literature Cited

(1) Kehiaian, H. V. *Pure Appl. Chem.* **1985**, *57*, 15.
(2) Garcia Vicente, I.; Garcia-Lisbona, N.; Velasco, I.; Otin, S.; Muñoz Embid, J.; Kehiaian, H. V. *Fluid Phase Equilib.* **1989**, *49*, 251.
(3) Wu, H. S.; Sandler, S. I. *AIChE J.* **1989**, *35*, 168.
(4) Kehiaian, H. V.; Marongiu, B. *Fluid Phase Equilib.* **1988**, *42*, 141.
(5) Kehiaian, H. V.; Marongiu, B. *Fluid Phase Equilib.* **1988**, *40*, 23.
(6) Berro, C.; Rogalski, M.; Péneloux, A. *Fluid Phase Equilib.* **1982**, *8*, 55.
(7) Berro, C.; Péneloux, A. *J. Chem. Eng. Data* **1984**, *29*, 206.
(8) Gutiérrez Losa, C.; Gracia, M. *Rev. Acad. Cienc. Exactas, Fis., Quim. Nat. Zaragoza* **1971**, *26*, 101.
(9) Velasco, I.; Otin, S.; Gutiérrez Losa, C. *Int. DATA Ser., Sel. Data Mixtures, Ser. A* **1979**, 8.
(10) Marsh, K. N. *Int. DATA Ser., Sel. Data Mixtures, Ser. A* **1973**, 22.
(11) Neau, E.; Péneloux, A. *Fluid Phase Equilib.* **1981**, *6*, 1.
(12) Fernández, J.; Berro, C.; Péneloux, A. *J. Chem. Eng. Data* **1987**, *32*, 17.
(13) Hayden, J. G.; O'Connell, J. P. *Ind. Eng. Chem. Process Des. Dev.* **1975**, *14*, 209.
(14) Wilhelm, E.; Faradjzadeh, A.; Grolier, J.-P. E. *J. Chem. Thermodyn.* **1979**, *11*, 979.
(15) López, J. A.; Pérez, P.; Gracia, M.; Gutiérrez Losa, C. *J. Chem. Thermodyn.* **1988**, *20*, 447.
(16) Young, H. D.; Nelson, O. A. *Ind. Eng. Chem.* **1932**, *4*, 67.
(17) Sagnes, M.; Sánchez, V. *J. Chem. Eng. Data* **1971**, *16*, 351.
(18) Rathbone, P. Presented at the 4th International IUPAC Conference on Chemical Thermodynamics, Montpellier, France, August 26-30, 1975; Paper VI/II.
(19) Azpiazu, Y.; Royo, F.; Gutiérrez Losa, C. *J. Chem. Thermodyn.* **1984**, *16*, 561.
(20) Kireev, V. A.; Skvortsova, A. A. *Zh. Fiz. Khim.* **1936**, *7*, 63.
(21) TRC Thermodynamic Tables. Non-hydrocarbons. Thermodynamics Research Center, The Texas A&M University System: College Station, TX, 1973, d-7240 and k-7240; 1981, d-7242; 1981, d-7040 and k-7040 (loose-leaf data sheets).
(22) Marongiu, B. *Int. DATA Ser., Sel. Data Mixtures, Ser. A* **1987**, 136.
(23) Marongiu, B. *Int. DATA Ser., Sel. Data Mixtures, Ser. A* **1988**, 2.
(24) Muñoz Embid, J.; Roux, A. H.; Grolier, J.-P. E. *Int. DATA Ser., Sel. Data Mixtures, Ser. A* **1990**, 59.
(25) Diguet, R.; Jadzyn, J. *J. Chem. Eng. Data* **1982**, *27*, 86.
(26) Vlj, J. N.; Mahl, B. S. *Thermochim. Acta* **1975**, *12*, 155.

Received for review September 26, 1989. Accepted February 23, 1990. S.O. and J.M.E. are grateful for the financial assistance of the Dirección General de Política Científica (Madrid, Spain) (PB 86-0184). J.M.E. greatly appreciates the financial assistance of the Ministère de la Recherche et de l'Enseignement Supérieur (France) and the Ministerio de Educación y Ciencia (Spain).

Solubility of Naphthalene in Mixtures of Carbon Dioxide and Ethane

William E. Hollar, Jr.,† and Paul Ehrlich*

Department of Chemical Engineering, State University of New York at Buffalo, Amherst, New York 14260

The solubility of naphthalene in supercritical mixtures of carbon dioxide and ethane has been measured at temperatures of 308 and 318 K and over a pressure range of 50-300 atm with a static solubility apparatus. The resulting solubility data were correlated with the Chueh-Prausnitz modified version of the Redlich-Kwong equation of state.

I. Introduction

A number of authors have investigated the solubility behavior of solid solutes in contact with a binary solvent mixture that is supercritical at the conditions of the experiment (*1-3*). With the exception of one study (*1*), each has examined a polar or nonpolar liquid entrainer (cosolvent) at levels of 3-10 mol % as the second component of the supercritical solvent mixture. Schmitt and Reid (*1*) measured the solubility of naphthalene and benzoic acid in a mixture of 94% CO_2-6% C_2H_6 at 308 and 318 K. These data are the only source of information on the

† Present address: The Carborundum Co., P.O. Box 832, Niagara Falls, NY 14302.

0021-9568/90/1735-0271$02.50/0

system naphthalene (1)–ethane (2)–carbon dioxide (3) in the literature.

The present study has focused on solubility measurements in solvent mixtures containing substantial amounts of both components. Since the component pure solvents are above their critical temperatures, solubility behavior at relatively low pressures can be examined without the potential problem of cosolvent condensation. The temperature, pressure, and composition coordinates (T, P, y) of the critical end points of the two binary systems, naphthalene–ethane and naphthalene–carbon dioxide, are a useful reference in an examination of the data for the ternary system. The value of y will be taken to represent the mole fraction of the solute (naphthalene) and hence its solubility in the supercritical phase. Each of the critical end points lies at an intersection of a three-phase solid–liquid–gas (S–L–G) equilibrium with the L–G critical locus (*4*, *5*), the first, U_1, quite close in temperature and pressure to the critical point of the pure solvent, implying a very small solute solubility, e.g., $y \sim 2 \times 10^{-3}$ for naphthalene–ethylene (*6*). The three S–L–G lines that emanate from the second critical end point, U_2, terminate at the triple point of the pure solute. The coordinates of U_2 may be estimated to lie at 60.1 °C and 252.7 atm for naphthalene–CO_2 (*7*) and at 56.5 °C, 122.5 atm, and 0.198 for naphthalene–ethane (*7*, *8*).

The two solvents, CO_2 and C_2H_6, have nearly identical critical temperatures, 31.1 and 32.3 °C, respectively, and their mixtures have a continuous critical locus, both of these features aiding a meaningful comparison between these two solvents. The solvent–solvent critical locus displays a minimum temperature of 28 °C at 57 mol % CO_2, accompanied by azeotrope formation (*9*). The two experimental temperatures chosen were 35 and 45 °C, and our experimental pressures of 58–300 atm encompass the range over which the isothermal solubility undergoes a large increase toward a plateau, characteristic of each temperature. Solubilities ranged from 3×10^{-4} to 3.6×10^{-2}, still several times smaller than those at U_2. While strongly synergistic effects, as occur with entrainers, were not expected with this binary nonpolar solvent mixture, it was of interest to determine the presence or absence of strongly nonlinear effects in mixtures containing substantial amounts of both solvents. We restricted ourselves to solvent composition equimolar or richer in C_2H_6, which is the better solvent.

The solubility data were modeled using the Chueh–Prausnitz version (*10*) of the Redlich–Kwong (RK) equation; solvent–solvent interaction parameters were regressed from the experimental data.

II. Experimental Section

Solubilities were measured in a static solubility apparatus, using a technique similar to the pellet disappearance method first developed by Tsekhanskaya et al. (*11*). Solvent mixtures of the desired composition were liquefied into the equilibrium vessel, which contained a known amount of naphthalene in the form of pellets. The system pressure was generated by heating the system to the desired temperature at constant density. The system was held at constant temperature and pressure until equilibrium was attained. The heating and equilibration process normally took 5–6 h, with the system being held at constant temperature and pressure for 2–3 h. At this point, the solubility of the solute was determined by measuring the change in mass of the naphthalene pellet(s). Measurements of naphthalene solubilities in pure carbon dioxide and ethane were performed to validate the experimental procedure. The experimental error of 14 solubility measurements in CO_2 at 45 °C and 60–110 atm from Tsekhanskaya's data, an often cited reference, was 11.1%. This error was larger than that of some other studies (*12*–*16*) and was associated with small solubilities and their large pressure and temperature coefficients. A smooth curve drawn through the experimental data at 75–110 atm was, however, nearly indistinguishable from that of Tsekhanskaya.

The temperature of the equilibrium vessel was determined by monitoring the constant-temperature bath with an iron–constantan thermocouple (accuracy of ±0.2 K). The standard deviation of the bath temperature was ±0.5 °C. The system pressure was monitored with a Baldwin-Lima-Hamilton strain gauge transducer to ±5 psi. Solvent densities were determined from a knowledge of the equilibrium vessel volume and the mass of solvent liquefied into the system. Solvent densities at equilibrium were determined from a knowledge of the vessel's volume corrected for that of the solute (*17*).

For the mixed solvent systems, 25 data points were obtained, each under a different set of conditions of temperature, pressure, and mixture composition. The accuracy of the individual measurements varied because of the wide range in solubilities and their pressure coefficients. An analysis of the quality of the data also depends on the empirical fit or equation of state chosen to represent them. In the linear regression analysis of the straight-line fit of the enhancement factor vs the solvent density at 35 °C, the standard error is 4.6% for the best case, CO_2, and 9.5% for the worst case, 39.9 mol % CO_2, with omission of the deviant point to be referred to (Figure 3).

The gases were purchased from Union Carbide, with a stated minimum purity of 99.0% for the ethane and 99.8% for the carbon dioxide. "Scintanalyzed" (liquid scintillation grade) naphthalene was purchased from the Fisher Scientific Co., Inc., and had a state minimum purity of 99.99%. All materials were used without subsequent purification.

Table I. Mixed Solvent Solubility Data: T = 308 K; $y(CO_2)$ = 0.496

pressure, atm	$y(C_{10}H_8) \times 10^4$	enhancement factor	density, g-mol/L	solvent composition $y(CO_2)$
57.9	2.8	56	4.0	0.480
72.5	10.5	265	6.6	0.528
77.4	33.4	895	9.0	0.483
82.3	48.0	1369	10.5	0.509
89.9	79.6	2477	11.7	0.500
110.7	123.7	4740	12.9	0.491
149.8	179.2	9293	14.5	0.505
173.8	216.2	13002	14.7	0.470

Table II. Mixed Solvent Solubility Data: T = 308 K; $y(CO_2)$ = 0.399

pressure, atm	$y(C_{10}H_8) \times 10^4$	enhancement factor	density, g-mol/L	solvent composition $y(CO_2)$
69.0	16.2	387	7.0	0.398
70.5	27.6	673	7.3	0.396
74.7	48.0	1241	9.5	0.413
103.6	118.0	4230	13.2	0.437
157.8	212.0	11576	14.0	0.386
203.6	274.0	19303	14.5	0.354
298.6	323.4	33373	15.5	0.408

Table III. Mixed Solvent Solubility Data: T = 318 K; $y(CO_2)$ = 0.474

pressure, atm	$y(C_{10}H_8) \times 10^4$	enhancement factor	density, g-mol/L	solvent composition $y(CO_2)$
57.9	5.0	42	3.5	0.480
76.1	19.0	210	6.3	0.465
98.3	99.1	1414	10.4	0.475
186.3	357.0	9653	14.3	0.477

III. Results and Discussion

Naphthalene solubility data in four mixtures of carbon dioxide and ethane are presented in Tables I–IV. Tables I and II list data measured at 308 K, while Tables III and IV contain data measured at 318 K. Each table lists naphthalene solubility,

Table IV. Mixed Solvent Solubility Data: T = 318 K; $y(CO_2)$ = 0.254

pressure,[a] atm	$y(C_{10}H_8) \times 10^4$	enhancement factor	density, g-mol/L	solvent composition $y(CO_2)$
68.1*	17.1	169	6.1	0.277
71.6*	47.3	492	7.3	0.251
73.4	28.9	309	7.0	0.292
83.2*	115.8	1398	10.3	0.219
107.6	219.6	3430	11.9	0.204
111.6*	211.8	3431	12.2	0.278

[a] The data points marked with an asterisk have been corrected for dead volume present in this set of experiments. The correction procedure has been detailed in Appendix B of ref 17.

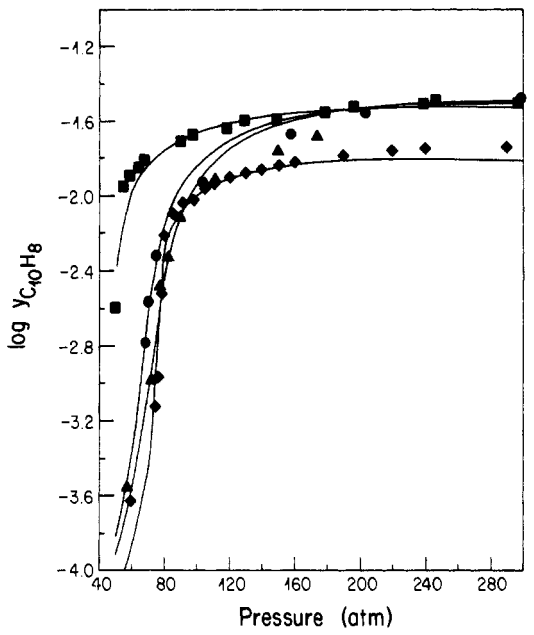

Figure 1. Naphthalene solubility versus pressure in pure ethane (■) (data of Schmitt and Reid (*18*)), pure carbon dioxide (♦) (data of Tsekhanskaya et al. (*11*)), and mixtures containing 39.9 (●) and 49.6 (▲) mol % CO_2 at a temperature of 308 K. Solid lines are the solubility isotherms as predicted by the RK equation of state.

pressure, solvent density, solvent composition, and the enhancement factor. The latter is defined as the ratio of the actual to the ideal Raoult's law solubility. Each solubility isotherm contains solubility data measured in solvent mixtures with a maximum composition variation of ±5 mol % relative to the average composition. The standard deviations in composition ranged from 0.6 to 3.2 mol %. These variations reflected experimental limitations in making up precisely predetermined solvent compositions, but the individual compositions are known to three significant figures (see tables). Use of an average solvent composition in the plots to be shown did not displace them significantly from those which would have been obtained, if each point had been corrected individually to the common average composition. A particular isotherm will, therefore, be referenced by its average solvent composition (determined on a solute-free basis).

Naphthalene solubility data for mixtures of 39.9 and 49.6 mol % CO_2 (on a solute-free basis) at 308 K are shown in Figure 1. The solubility of naphthalene in pure carbon dioxide (Tsekhanskaya et al. (*11*)) and naphthalene in pure ethane (Schmitt and Reid (*18*)) have been included for comparison. Three main features of interest can be seen on this plot. The rate of solubility increase with increasing pressure is lower for the solvent mixture than for either pure component in the near-critical region. This behavior changes at higher pressures, where $dy(\text{solute})/dP$ is greater in the solvent mixture. Further, the solvating power of both solvent mixtures is similar to that

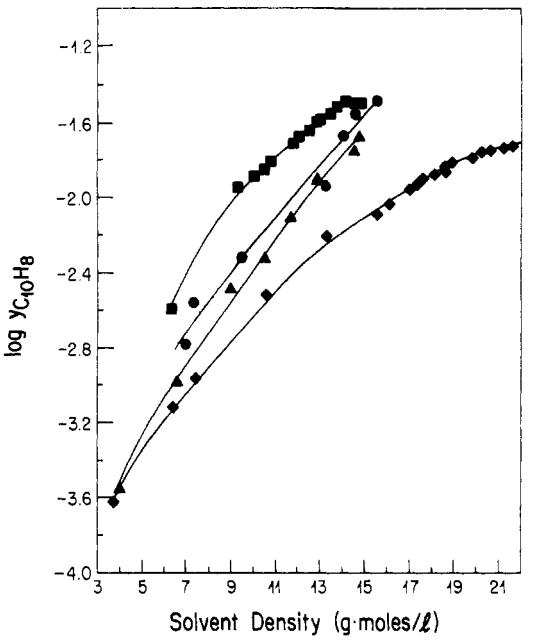

Figure 2. Naphthalene solubility as a function of solvent density in pure ethane (■) (data of Schmitt and Reid (*18*)), pure carbon dioxide (♦) (data of Tsekhanskaya et al. (*11*)), and mixtures of 39.9 (●) and 49.6 (▲) mol % CO_2. T = 308 K.

of pure carbon dioxide, when examined at near-critical pressures. As the pressure levels become higher, the influence of the ethane in the mixture becomes more apparent. This is demonstrated by the asymptotic approach of the solubilities in the mixtures toward the limiting value in the pure ethane. At the highest pressure (300 atm), the solubility in the 40% CO_2 mixture actually exceeds the solubility in the pure ethane.

The solubility behavior in the equimolar mixture over the pressure range of 80–100 atm is particularly interesting. The solubility of $C_{10}H_8$ in the mixture lies below the solubilities in both of the component pure solvents, and this is apparently a result of lowered densities for the mixture compared to the pure solvents over this limited pressure range. This behavior was not found for the 40% mixture.

Figure 2 shows the same solubility data plotted as a function of the solvent density. As in other cases, a simpler behavior is found when solubilities are compared at constant solvent density (*19*). At low densities, the solubilities in the mixtures lie closer to the levels found in pure CO_2; however, as the density is increased, the influence of the ethane in the mixture becomes more important.

Figure 3 illustrates the variation of the enhancement factor with the solvent density at 308 K for both the pure solvents and their mixtures. For the 50% mixture, the logarithm of the enhancement factor varies linearly with the solvent density. The 40% mixture shows a similar trend, particularly if the single data point at intermediate density is ignored. The experimental value of the density for this data point appeared to be too high. Thus, the solvent mixtures exhibit behavior typical of pure solvents (*13*).

The solubility at 318 K is plotted as a function of pressure in Figure 4. Solubility data for naphthalene in a 47.4% CO_2 mixture, a 25.4% CO_2 mixture, pure ethane (data of Schmitt and Reid (*18*)), and pure carbon dioxide (data of Tsekhanskaya et al. (*11*)) are shown. The increased ethane content of the 25% mixture shifts the solubilities to levels more typical of the pure ethane. The solubility behavior in the 50% mixture is similar to that at the lower temperature, in that the low-pressure solubilities are most strongly influenced by the carbon dioxide. At elevated pressures (>120 atm), the solubility in the mixture begins to approach the pure ethane solubilities.

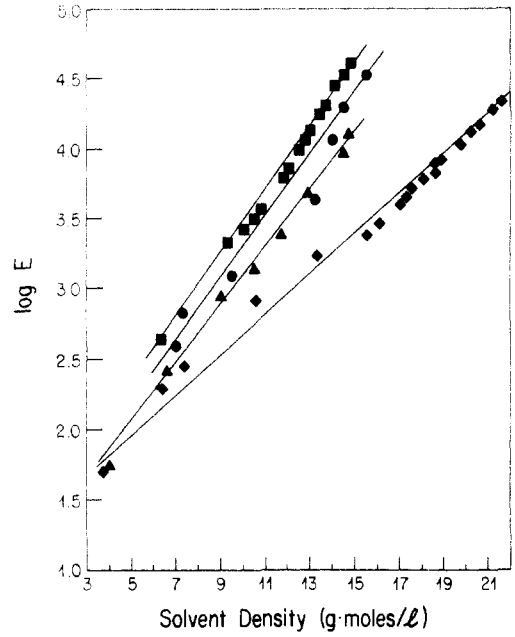

Figure 3. Enhancement factor versus solvent density for carbon dioxide (♦) and ethane (■) (data from refs 11 and 18) and 39.9 (●) and 49.6 (▲) mol % carbon dioxide at 308 K.

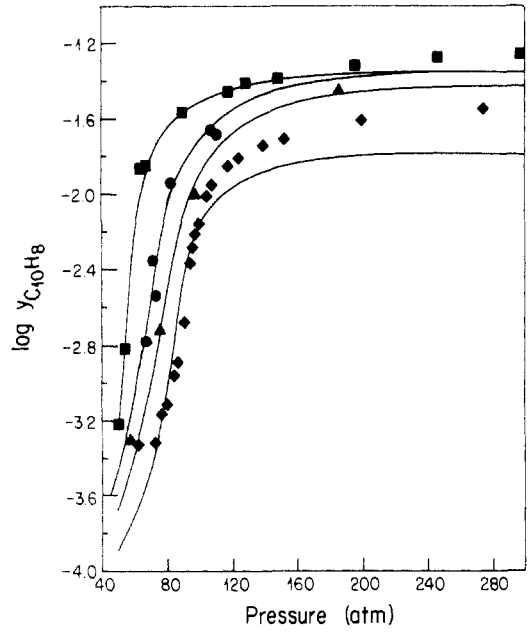

Figure 4. Naphthalene solubility versus pressure for pure ethane (■) (data of Schmitt and Reid (*18*)), pure carbon dioxide (♦) (data of Tsekhanskaya et al. (*11*)), and mixtures containing 25.4 (●) and 47.4 (▲) mol % CO_2 at a temperature of 318 K. Solid lines are the RK equation of state predicted solubilities at each solvent composition.

The effect of temperature on the solubility in the solvent mixture was examined by using the equimolar mixture solubility data at 35 and 45 °C; Figure 5 shows the solubility as a function of pressure for the equimolar mixtures. The existence of a crossover point (*21*) can be seen at a pressure of approximately 100 atm; this is one demonstration of the similarity between the solubility behavior of pure and mixed gas supercritical solvents. In a pure solvent, higher solubilities occur as the temperature is increased at constant density (*4*). This type of behavior is also manifested by the solvent mixture (*17*).

The solubility data have been correlated with use of the Chueh–Prausnitz mixing rules for the Redlich–Kwong equation of state. Solvent–solvent interaction parameters have been determined from mixed gas solubility data; this calculation necessitated a knowledge of the solute–solvent interaction pa-

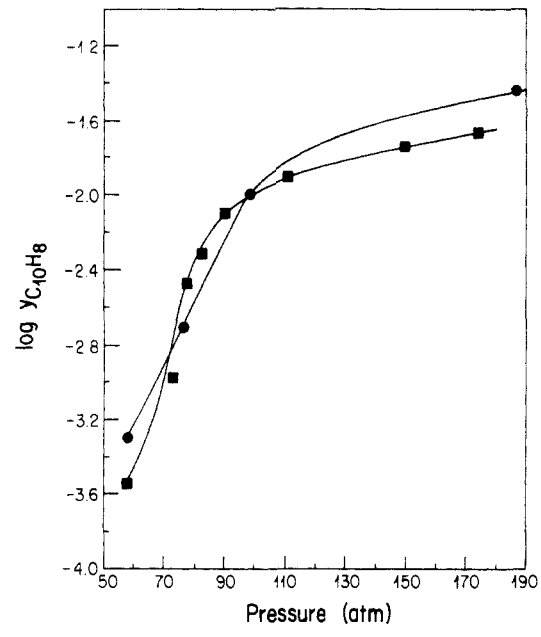

Figure 5. Effect of temperature on the naphthalene solubility–pressure in "equimolar" solvent mixtures: T = 308 K (■) and 318 K (●).

Table V. Binary Solvent–Solute Interaction Parameters

solvent	temp., K	k_{ij}	AAD[a]	source
C_2H_6	308	0.009	0.127	Schmitt and Reid (*18*)
	318	0.004	0.108	
	328	0.000	0.324	
CO_2	308	0.079	0.381	Tsekhanskaya et al. (*11*)
	318	0.088	0.302	
	328	0.085	0.310	

[a] Absolute average derivation.

Table VI. Solvent–Solvent Interaction Parameters

solvent composition	temp	k_{23}	AAD	source
0.399	35	0.089	0.096	this study
0.496	35	0.108	0.191	this study
0.9383	35	0.130	0.047	Schmitt and Reid (*1*)
0.254	45	0.099	0.184	this study
0.474	45	0.079	0.138	this study
0.9383	45	0.460	0.304	Schmitt and Reid (*1*)
			0.160[a]	

[a] The average AAD (absolute average deviation) for the first five isotherms was 0.131.

rameters for the binary systems $C_{10}H_8$ (1)–C_2H_6 (2) and $C_{10}H_8$ (1)–CO_2 (3). All interaction parameters were determined by minimization of the absolute average deviation (*20*). The solute–solvent interaction parameters are summarized in Table V. Table VI summarizes the solvent–solvent interaction parameters for the four solubility isotherms measured in this study. In addition, the data of Schmitt and Reid (*1*) ($y(CO_2)$ = 0.94) have been examined with this analysis. A comparison of predicted and experimental solubility data is shown in Figures 1 and 4. The Redlich–Kwong equation of state predicts the mixed gas solvent solubility behavior best at near-critical and elevated pressure levels, with increasing deviations at intermediate pressure levels.

The solvent–solvent interaction parameter does not appear to be a strong function of composition. For five of the six isotherms, the value of this parameter varied from 0.08 to 0.13. Since variations of this magnitude in this parameter produce only minor changes in the predicted solubilities, the parameter (to a first approximation) may be considered effectively constant. Of further interest is the fact that the magnitude of this

Table VII. Observed and Calculated Solubilities

temp, K	$y(CO_2)$	pressure, atm	$y_{C_{10}H_8}$ obs	$y_{C_{10}H_8}$ calc	% error
308	0.201	239.1	0.0308	0.0323	4.9
308	0.950	98.7	0.00957	0.00972	1.6
318	0.393	139.1	0.02546	0.02955	16.1
31	0.103	60.1	0.00150	0.00133	11.3
318	0.570	93.4	0.00586	0.00515	12.1
					9.2[a]

[a] Average value.

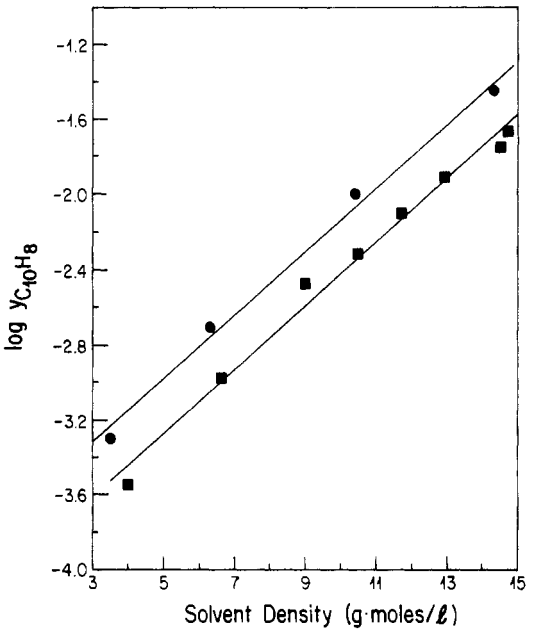

Figure 6. Comparison of predicted and experimental solubility data: mixed solvent solubility data at 308 K (■) and 318 K (●).

parameter (k_{23} = 0.1) is similar to the value for the ethane–carbon dioxide system predicted from virial coefficient data (*23*). This appears to indicate that, at least for weakly interacting solvent pairs, semiquantitative predictions of mixed gas solubility behavior can be obtained from a knowledge of binary solute–solvent interactions used in tandem with solvent–solvent interaction parameters from the literature.

To test this hypothesis, single solubility data points not associated with the solubility isotherms presented earlier were modeled with use of solvent–solvent interaction parameters predicted from the isotherms. The single solubility data points are listed in Table VII; these measurements were performed over a wide range of solvent compositions and pressures in order to better map out the composition effect on solubility. Figure 6 compares the calculated and actual solubilities based on the single solubility data points. The solubilities were predicted to an average error of 9%. The success of this extrapolation is an indication that, for this type of system, solubility data over a range of solvent compositions can be successfully modeled with solvent–solvent interaction parameters regressed from data of limited composition range.

Registry No. CO_2, 124-38-9; C_2H_6, 74-84-0; naphthalene, 91-20-3.

Literature Cited

(1) Schmitt, W.; Reid, R. C. Fluid Phase Equilib. **1986**, *32*, 77.
(2) Van Alsten, J. G.; Hansen, P. C.; Eckert, C. A. Supercritical Enhancement Factors for Non-polar and Polar Systems. Presented at the 1984 AIChE National Meeting, San Francisco, CA, 1984; Paper 84a.
(3) Dobbs, J. M.; Wong, J. M.; Johnston, K. P. *J. Chem. Eng. Data* **1986**, *31*, 303.
(4) Paulaitis, M. E.; Krukonis, V. J.; Kurnik, R. T.; Reid, R. C. *Rev. Chem. Eng.* **1983**, *1*, 179.
(5) Koningsveld, R.; Diepen, G. A. M. *Fluid Phase Equilib.* **1983**, *10*, 159.
(6) Diepen, G. A M.; Scheffer, F. E. C. *J. Phys. Chem.* **1953**, *57*, 575.
(7) McHugh, M. A.; Yogan, T. J. *J. Chem. Eng. Data* **1984**, *29*, 112. See also: McHugh, A. M.; Krukonis, V. J. *Supercritical Fluid Extraction: Principles and Practice*; Butterworth: Boston, 1986.
(8) van Welie, G. S. A.; Diepen, G. A. M. *J. Phys. Chem.* **1963**, *67*, 755.
(9) Kuenen, J. P. *Philos. Mag.* **1897**, *44*, 174. Ohgaki, K.; Katayama, T. *Fluid Phase Equilib.* **1977**, *1*, 27.
(10) Chueh, P. L.; Prausnitz, M. M. *Ind. Eng. Chem. Fundam.* **1967**, *6*, 492.
(11) Tsekhanskaya, Y. V.; Iomtev, M. B.; Mushkina, E. V. *Russ. J. Phys. Chem.* **1964**, *38*, 1173.
(12) McHugh, M. A.; Paulaitis, M. E. *J. Chem. Eng. Data* **1978**, *23*, 326.
(13) Johnston, K. P.; Ziger, D. H.; Eckert, C. H. *Ind. Eng. Chem. Fundam.* **1982**, *21*, 191.
(14) Chang, H.; Morrell, D. G. *J. Chem. Eng. Data* **1985**, *30*, 74.
(15) Kurnik, R. T.; Holla, S. J.; Reid, R. C. *J. Chem. Eng. Data* **1981**, *26*, 47.
(16) Tan, C.-S.; Weng, J. Y. *Fluid Phase Equil.* **1987**, *34*, 37.
(17) Hollar, W. E. The Solubility of Naphthalene in Mixtures of Carbon Dioxide and Ethane. Ph.D. Dissertation, State University of New York at Buffalo, 1988.
(18) Schmitt, W. J.; Reid, R. C. *J. Chem. Eng. Data* **1986**, *31*, 204.
(19) Allada, S. R. *Ind. Eng. Chem. Process Des. Dev.* **1984**, *23*, 344.
(20) Schmitt, W.; Reid, R. C. The Influence of the Solvent Gas on Solubility and Selectivity in Supercritical Extraction. Paper presented at the AIChE National Meeting, San Francisco, CA, 1984.
(21) Chimowitz, E. H.; Pennisi, K. J. *AIChE J.* **1986**, *32*, 1665.
(22) Wong, J. M.; Pearlman, R. S.; Johnston, K. P. *J. Phys. Chem.* **1985**, *89*, 2671.
(23) Prausnitz, J. M.; Lichtenthaler, R. N.; Azevedo, E. G. *Molecular Thermodynamics of Fluid Phase Equilibria*; Prentice-Hall: Englewood, NJ, 1986.

Received for review November 28, 1988. Revised October 27, 1989. Accepted February 13, 1990.